



Available online at www.sciencedirect.com

ScienceDirect

Geochimica et Cosmochimica Acta 317 (2022) 472-487

Geochimica et Cosmochimica Acta

www.elsevier.com/locate/gca

Phylogeny, alkenone profiles and ecology of Isochrysidales subclades in saline lakes: Implications for paleosalinity and paleotemperature reconstructions

Yuan Yao ^{a,b,c}, Jiaju Zhao ^b, Richard S. Vachula ^d, Sian Liao ^e, Gaoyuan Li ^f, Emma J. Pearson ^g, Yongsong Huang ^{c,*}

^a Institute of Global Environmental Change, Xi'an Jiaotong University, Xi'an 710054, China

^b State Key Laboratory of Loess and Quaternary Geology, Institute of Earth Environment, Chinese Academy of Sciences, Xi'an 710061, China

^c Department of Earth, Environmental and Planetary Sciences, Brown University, Providence, RI 02912, USA

^d Department of Geology, College of William and Mary, Williamsburg, VA 23185, USA

^e Department of Chemistry, Brown University, Providence, RI 02912, USA

^f State Key Laboratory of Biogeology and Environmental Geology, China University of Geosciences, Beijing 100083, China

^g School of Geography, Politics and Sociology, Newcastle University, Newcastle-upon-Tyne, NE1 7RU, UK

Received 17 May 2021; accepted in revised form 1 November 2021; Available online 9 November 2021

Abstract

Long-chain alkenones (LCAs) produced by phylogenetically classified Groups 1 and 3 Isochrysidales are increasingly used for paleotemperature and/or paleosalinity reconstructions in oligonaline lakes and marine environments. However, there are considerable difficulties in the paleoenvironmental interpretation of LCAs from Group 2 Isochrysidales thriving in saline lakes. The biggest challenge lies in our poor understanding of the complexity and ecological niches of individual Group 2 subclades in saline lakes. Here, we perform comprehensive analysis of haptophyte-specific 18S rRNA sequences and distributions of LCAs, and long-chain alkenoates (LCEs) in surface sediments and suspended particulate matter (SPM) from 37 saline lakes in northern China. These lakes span a large salinity gradient from 0.5 to 308%. Combined with published genomic data of Group 2 Isochrysidales, our phylogenetic analysis reveals three Group 2 subclades occupying distinct ecological niches: one ice-related bloomer Group 2i and two warm-season bloomers Groups 2w1 and 2w2. Group 2i, the earliest seasonal bloomer, frequently co-occurs with Group 2w1 in sediments from saline lakes with relatively low to intermediate salinity waters, whereas Group 2w2 blooms in hypersaline waters. Based on existing data, C_{39:4} methyl alkenone is a chemotaxonomic biomarker for Group 2i. %C_{37:4} (relative abundance of C_{37:4} to the total C₃₇ alkenones) values in the three Group subclades follow the order: Group 2i > Group 2w2 > Group 2w1. The $\%C_{37.4}$ in sediment cores of saline lakes does not directly record past salinity changes, but instead reflects variable contributions in production by these three subclades. This could indirectly and partially reflect overall salinity changes in some lakes dominated by Groups 2i and 2w1, but can be more complicated in lakes dominated by other assemblages. For our sites, we also demonstrate that direct use of C₃₇ alkenone unsaturation indices (U_{37}^K, U_{37}^K) , and $U_{37}^{K'}$) for paleotemperature reconstructions in saline lakes is generally not feasible, except for cases where alkenone-producing Isochrysidales are dominated by one single species/subclade and seasonal production effects can be circumvented. We propose two possible alternative proxies for paleotemperature reconstructions in saline lakes: 1) unsaturation ratios of C₄₁ and C₄₂ alkenones, as these compounds are predominantly produced by a limited number of Group 2 species, such as Isochrysis nuda (Liao et al., 2020); 2) C₃₈Et/C₃₆OEt ratio (ratio of C₃₈ ethyl alkenones and C₃₆ ethyl alkenoates), which appears to have similar temperature sensitivity for Groups 2w1 and 2w2, in lakes with no Group 2i inputs. Our study provides new insights into the phylogenetic classifications of Group 2 Isochrysidales and their ecological/environmental

^{*} Corresponding author at: Department of Earth, Environmental and Planetary Sciences, Brown University, Providence, RI 02912, USA. *E-mail address:* yongsong_huang@brown.edu (Y. Huang).

niches, which are fundamental for more quantitative and rigorous applications of LCAs and LCEs in saline lakes as pale-osalinity and paleotemperature proxies.

© 2021 Elsevier Ltd. All rights reserved.

Keywords: Alkenones; Alkenoates; Group 2 Isochrysidales; Paleosalinity proxy; Paleotemperature proxy; Saline lakes

1. INTRODUCTION

Long-chain alkenones (LCAs) are a class of C₃₅-C₄₂ di-, tri- and tetra-unsaturated methyl (Me) and ethyl (Et) ketones, with C₃₇ methyl (C₃₇Me) and C₃₈ ethyl (C₃₈Et) chain lengths appearing as the most common and abundant alkenones in marine and lake environments (e.g., Brassell et al., 1986; Zink et al., 2001; Chu et al., 2005; Conte et al., 2006; Longo et al., 2018). They are exclusively produced by certain Isochrysidales species within haptophyte lineages, such as Emiliania huxleyi and Gephyrocapsa oceanica in open marine environments (e.g., Volkman et al., 1980; Marlowe et al., 1984), non-calcifying Isochrysis galbana, Ruttnera (Chrysotila) lamellosa, Isochrysis nuda, and Isochrysis litoralis in saline lakes and/or coastal seas (e.g., Sun et al., 2007; Nakamura et al., 2014; Zheng et al., 2016, 2019; Liao et al., 2020), as well as the more recently discovered (uncultured) species living in fresh and oligohaline waters (D'Andrea and Huang, 2005; D'Andrea et al., 2006; Theroux et al., 2010). Numerous laboratory culture and natural sample studies have demonstrated that C_{37} alkenone unsaturation indices $(U_{37}^K,\,U_{37}^{K'},\,$ and $U_{37}^{K''}$) have strong correlations with temperatures in cultured Isochrysidales species (e.g., Prahl and Wakeham, 1987; Conte et al., 1998; Sun et al., 2007; Nakamura et al., 2014; Zheng et al., 2016, 2019; Araie et al., 2018) and in marine and certain lake environments (e.g., Zink et al., 2001; Conte et al., 2006; D'Andrea et al., 2011, 2016; Longo et al., 2016). In particular, the $U_{37}^{K''}$ values, which exclude the di-unsaturated alkenone, strengthen temperature correlations for some non-calcifying Isochrysidales species (Zheng et al., 2016; Liao et al., 2020). These unsaturation indices have been widely and successfully used to reconstruct past sea surface temperatures (SST) for more than 30 years (e.g., Brassell et al., 1986; Prahl and Wakeham, 1987; Eglinton et al., 1992), and were subsequently adapted for application to lake sedimentary records (e.g., Liu et al., 2006; D'Andrea et al., 2011; He et al., 2013; Hou et al., 2016; Zhao et al., 2017; Longo et al., 2020).

Following the introduction of 18S rRNA sequencing methods for Isochrysidales identification in sediment samples (Coolen et al., 2004), numerous phylogenetic analyses have revealed that alkenone-producing Isochrysidales are composed of three phylogenetically distinct groups: Group 1, Group 2, and Group 3 (Theroux et al., 2010; Longo et al., 2016; D'Andrea et al., 2016; Araie et al., 2018; Plancq et al., 2019; Yao et al., 2019). Group 1 Isochrysidales contain two subclades (Richter et al., 2019): Group 1a (formerly "Greenland" subclade; D'Andrea et al., 2006; Theroux et al., 2010) and Group 1b (formerly "EV" subclade; Simon et al., 2013; Richter et al., 2019). These

Groups occupy different habitats, with Group 1 occurring freshwater/oligohaline lakes (defined here as salinity < 6%), Group 2 in brackish/saline lakes (salinity > 6 %), coastal seas and/or sea ice environments, and Group 3 in open ocean environments (Longo et al., 2016; Yao et al., 2020; Wang et al., 2021). In freshwater lakes, the distinctive Group 1-type LCAs produced by Group 1 Isochrysidales are characterized by the presence of tri-unsaturated isomers with $\Delta^{14,21,28}$ (C_{37:3b}) double bond positions (in addition to the common $\Delta^{7,14,21}$ (C_{37:3a}) in Groups 2 and 3 Isochrysidales; Longo et al., 2013, 2016; Dillon et al., 2016; Zheng et al., 2019). Group 1 LCAs have great potential for quantitative reconstructions of cold season temperatures (Longo et al., 2018; Yao et al., 2019) due to the maximum production of Group 1 LCAs during lake ice melt and isothermal mixing (D'Andrea et al., 2011, 2016; Longo et al., 2018). In saline lakes, however, the diversity of Group 2 Isochrysidales hampers the direct use of alkenones as a paleotemperature proxy (Theroux et al., 2010; Randlett et al., 2014). Both variable temperature calibrations for alkenones from different Group 2 species/ strains (e.g., Wang et al., 2015; D'Andrea et al., 2016; Zheng et al., 2019) and different growth seasons of various Group 2 genotypes (Zhao et al., 2018; Theroux et al., 2020) contribute to the difficulty. In fact, two phylogenetically distinct Group 2 genotypes (OTU 7 or Hap-A and OTU 8 or Hap-B; Theroux et al., 2010; Toney et al., 2012) have been found to occur in some saline lakes in China and North America (Theroux et al., 2010). They have different bloom timings, with OTU 8 (Hap-A) blooming during spring and OTU 7 (Hap-B) blooming during summer (Theroux et al., 2020). However, the temperature sensitivities (i.e., slopes of temperature calibrations) of alkenone unsaturation indices are similar for Hap-A and Hap-B based on analysis of suspended particulate matter (SPM) samples collected over the seasonal cycle (Toney et al., 2010; Theroux et al., 2020). The seasonality of LCA production thus creates additional complexities for quantitative paleotemperature reconstructions using alkenone unsaturation indices, but may also provide an opportunity for understanding seasonality signals, as previously demonstrated by Zhao et al. (2018). The shifts in production of different season-blooming Group 2 species/subclades and the resulting changes in %C_{37:4} (abundance of C_{37:4} relative to the total C₃₇ alkenones) have been interpreted as an effective proxy for reconstructing winter-spring precipitation, rather than temperature changes, in a sediment core from Lake Gahai on the Qinghai-Tibetan plateau (Zhao et al., 2018).

In addition to temperature, the ratios of different alkenones also have the potential to provide salinity information. Recent studies have demonstrated that the RIK₃₇

(ratio of isomeric ketones of C₃₇ chain length) index (Longo et al., 2016) can be used as a reliable paleosalinity proxy in oligohaline environments with mixed Groups 1 and 2 Isochrysidales (Kaiser et al., 2019; Yao et al., 2020, 2021; Huang et al., 2021), due to the gradual transition from Group 1 to Group 2 with increasing salinity (salinity < ~6 ‰; Yao et al., 2020; note that this threshold value may change slightly as Isochrysidales DNA data from lakes is continually updated in the future). In saline lakes, $\%C_{37.4}$ index has been proposed as a salinity indicator on the northern Qinghai-Tibetan Plateau, with higher %C_{37:4} corresponding to lower salinity (Liu et al., 2008; 2011). However, it has subsequently been found that there is no significant relationship between %C_{37:4} and salinity in other saline lake regions, such as the interior of the United States (Toney et al., 2010), northwestern China (Song et al., 2016), Canada (Plancq et al., 2018), and mid-latitude Asia (He et al., 2020). These observations suggest that the applications of LCAs as paleosalinity and paleotemperature proxies in saline lakes are likely hampered by a major lack of fundamental knowledge on the diversity and ecological/environmental niches of Group 2 clades/subclades.

In this study, we investigate LCA and long-chain alkenoate (LCE) distributions, as well as their producer 18S rRNA sequences, in surface sediment and SPM samples collected from 37 saline lakes spanning a wide salinity range (0.5–308‰) throughout northern China. We combine our data with previously published DNA sequences of Group 2 Isochrysidales (Coolen et al., 2004, 2009; Theroux et al., 2010; Hou et al., 2014; Araie et al., 2018; Plancq et al., 2019; Wang et al., 2021) to classify Group 2 subclades phylogenetically. Our main objectives are to 1) determine environmental controls on the ecological niches

of different Group 2 subclades; 2) identify chemotaxonomic signatures of LCAs and LCEs among different Group 2 subclades; 3) disentangle the potential factors influencing paleotemperature and paleosalinity proxies based on LCAs and LCEs in saline lakes.

2. MATERIALS AND METHODS

2.1. Study sites and samples

We collected surface sediment and SPM samples from 37 saline lakes in northern China during the summer of 2017 (Fig. 1). Surface sediments were retrieved using a grab-type sediment sampler (JSD-KH201), and the top ~ 2 cm of the sediments (here defined as surface sediments) were collected and transferred to NASCO Whirl-Pak bags for LCA and DNA analysis. SPM samples were filtered through Whatman GF/F filter (0.7 µm) using ~ 1-12L of lake water for LCA analysis. Another set of SPM samples was filtered through Millipore SVGPL10RC Sterivex-GP filter (0.22 µm) and then was saved in cell lysis buffer for DNA analysis. All collected samples were kept in a cooler with gel ice packs in the field. Then the samples for DNA analysis were frozen at -80 °C in the laboratory, and the samples for LCA analysis were frozen at -20 °C in the laboratory. Water temperature, pH, and salinity were measured simultaneously with a HACH Hydrolab water analyzer in the field. Although one-time measurements of salinity during the field campaign cannot capture the full-scale seasonal variations in our study lakes, our measured salinity could still be used for comparison of saline lakes that span a large salinity gradient.

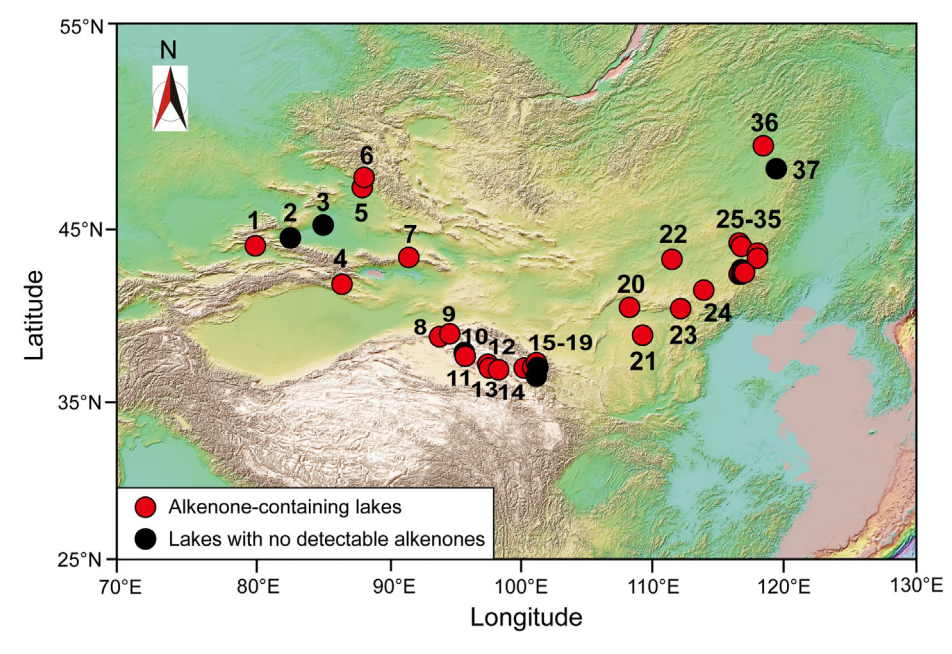


Fig. 1. Topographic map showing the sampling lake sites in northern China. Geographic information data are from the CGIAR Consortium for Spatial Information (CGIAR-CSI), http://srtm.csi.cgiar.org/SELECTION/inputCoord.asp. The LCA-containing lakes are marked with red circles and the lakes with no detectable LCAs are marked with black circles.

2.2. LCA and LCE analysis

All Chinese saline lake samples for LCA and LCE analysis were freeze-dried and extracted by sonication $(3 \times)$ with dichloromethane (DCM)/methanol (MeOH) (9:1, v/v). The extracts were purified by column chromatography with silica gel using n-hexane and dichloromethane (DCM), respectively. The DCM fractions were further purified by column chromatography with silver thiolate silica (Aponte et al., 2013; Wang et al., 2019). A sequence of solvents (hexane: DCM (2 ml, 2:1, v:v), DCM (1 ml), acetone (2 ml)) with increasing polarity was used to separate compounds. All LCAs and LCEs were retained in the acetone fractions (Zheng et al., 2017; Wang et al., 2019). LCAs and LCEs were then analyzed by an Agilent 7890 N GC system equipped with a flame ionization detector (FID) and a Restek Rtx-200 GC column (105 m \times 250 μ m \times 0.25 μ m) at Brown University, USA, as described by Zheng et al. (2017). Prior to the analysis, a known amount of 18-pentatricontanone was added to each sample as an internal standard for the quantification of LCAs and LCEs. The following GC-FID oven program was used: initial temperature of 50 °C (hold 2 min), ramp 20 °C /min to 255 °C, ramp 3 °C /min to 320 °C (hold 25 min). The carrier gas (H₂) was held at a constant flow rate of 1.5 mL/min under the flow pressure of $\sim 38-70$ psi. The 14 neutral fraction samples containing LCAs from the surface sediments of Spanish saline lakes (Pearson et al., 2008) were reanalyzed using the new GC method (Zheng et al., 2017). Note that this fraction had been saponified, which removed LCEs (Pearson et al., 2008).

The U_{37}^K (Brassell et al., 1986), $U_{37}^{K'}$ (Prahl and Wakeham, 1987), $U_{37}^{K''}$ (Zheng et al., 2016), C_{37} Me/ C_{38} Et, % $C_{37:4}$ (Rosell-Melé, 1998), and % $C_{39:4}$ Me are calculated as follows:

$$U_{37}^{k} = (C_{37:2} - C_{37:4})/(C_{37:2} + C_{37:3} + C_{37:4})$$
 (1)

$$U_{37}^{k'} = C_{37:2}/(C_{37:2} + C_{37:3}) (2)$$

$$U_{37}^{K''} = C_{37:3} / (C_{37:3} + C_{37:4}) (3)$$

 $C_{37}Me/C_{38}Et = (C_{37:2} + C_{37:3} + C_{37:4})/(C_{38:2}Et$

$$+ C_{38:3}Et + C_{38:4}Et) (4)$$

$$\%C_{37:4} = (C_{37:4}/(C_{37:2} + C_{37:3} + C_{37:4})) \times 100$$
 (5)

$$\%C_{39;4}Me = (C_{39;4}Me/(C_{39;2}Me + C_{39;3}Me + C_{39;4}Me)) \times 100$$

(6)

2.3. 18S rRNA analysis

DNA was extracted from ~ 0.5 g sediment subsamples from the Chinese saline lakes using the FastDNA SPIN Kit (MP Biomedicals, OH, USA) according to the manufacturer's instructions. Procedures of extraction, amplification, and cloning of DNA followed Yao et al. (2019). The haptophyte-specific oligonucleotide primers (Prym-429F: 5 $^\prime$ -GCG CGT AAA TTG CCC GAA-3 $^\prime$; Prym-887R: 5 $^\prime$ -GGA ATA CGA GTG CCC CTG AC -3 $^\prime$) were used for the amplification of targeted 18S rRNA (Coolen et al., 2004). A blank control was included in all of the

above steps, which serves as a control for cross-contamination during the experiments. The DNA experiments were performed at State Key Laboratory of Biogeology and Environmental Geology, China University of Geosciences (Beijing), China.

All obtained DNA sequences were analyzed through Basic Local Alignment Search Tool (BLAST) queries against the National Center for Biotechnology Information (NCBI) database (http://blast.ncbi.nlm.nih.gov/Blast.cgi) after removal of vector sequences. The operational taxonomic units (OTUs) of all trimmed sequences were determined using the DOTUR software program (Schloss and Handelsman, 2005) with a 98% similarity cut-off (Simon et al., 2013; Yao et al., 2019). Representative sequences for each OTU were chosen and aligned with reference haptophyte sequences from the GeoBank database for phylogenetic tree construction. The neighbor-joining tree was constructed using the molecular evolutionary genetics analysis (MEGA) software with 1000 bootstrap replications. The representative sequences for each OTU in this study have been deposited in GenBank (Accession numbers: OK298476-OK298479).

2.4. Statistical analyses

Based on the genomic data, logistic regressions between Group 2 subclades and water chemistry parameters were applied to determine the strength of environmental controls on the presence and absence of different Group 2 subclades using MATLAB. Redundancy analysis (RDA) was performed using the Canoco software version 4.5, in order to investigate environmental controls on the relative abundance of different Group 2 subclades.

2.5. Meteorological data

Monthly temperature data for all sites in this study were extracted from the WorldClim-Global Climate Database (http://www.worldclim.org/version2; Fick and Hijmans, 2017) with 30 seconds (~1km²) spatial resolution using the Senckenberg data extraction tool (dataportalsenckenberg.de/dataExtractTool).

3. RESULTS

3.1. The 18S rRNA-based Isochrysidales identification

Of the 37 Chinese saline lakes investigated in this study, surface sediment samples (n=29) of 29 lakes and SPM samples (n=16) of 14 lakes contain detectable LCAs (Tables S1 and S2). In the corresponding LCA-containing samples, the Isochrysidales DNA sequences from 15 surface sediment and 8 SPM samples are recovered using the haptophyte-specific primers from Coolen et al. (2004) (Table S3). The samples with no Isochrysidales DNA amplification may have low abundance of Isochrysidales DNA compared to the total community DNA and/or have poor DNA preservation. We identify four OTUs, which are defined as groups of DNA sequences with more than 98%

similarity, from all obtained 577 alkenone-producing Isochrysidales 18S rRNA sequences (Table S3). The two OTUs are grouped with previously published OTUs 7 and 8 from some saline lakes in China and North America (Theroux et al., 2010) at 98% similarity cut-off. Two new OTUs are found in this study, and classified as OTUs 9 and 10. For the sediment samples, the OTUs 7, 8, and 9 are three common Isochrysidales genotypes and occur as the assemblages of variable proportions (Fig. 2). The OTU 10 is only found in two lakes (Balikun and Haiyanwan), with Balikun predominantly containing the genotype (76%; Fig. 2). In the lake water samples collected in summer, we find the occurrence of three OTUs (OTUs 7, 9 and 10), with OTUs 7 and 9 being two common genotypes (Fig. S1). However, we did not capture OTU 8 in the summer lake water samples (Fig. S1).

We reconstructed the neighbor-joining phylogenetic tree of haptophyte 18S rRNA sequences using the representative sequences for each OTU along with 97 haptophyte DNA sequences from the NCBI and next-generation sequencing (NGS) database (Fig. 3). Our phylogenetic analysis includes the published 59 Group 2 DNA sequences from natural samples (3 sediment cores from Ace Lake, Black Sea, and Kusai Lake (Coolen et al., 2004, 2009; Hou et al., 2014): 10 surface sediment samples (salinity: 1.67-25.2%) from saline lakes (Table S4; Theroux et al., 2010; Plancq et al., 2019); 3 surface sediment samples from the Canadian Arctic Archipelago and 8 sea ice/water samples (Wang et al., 2021)) and representative isolated Group 2 species (I. galbana, I. litoralis, I. nuda, R. lamellosa, and unclassified strain Sh1, Sc2 and Dm2 (Araie et al., 2018) and RCC5486 (Wang et al., 2021)). All of our defined OTUs 7-10 are affiliated with Group 2 Isochrysidales. The OTUs 7 and 10 are phylogenetically related to

I. galbana, I. litoralis, and I. nuda species, but the OTUs 8 and 9 are not closely related to any named Group 2 species.

3.2. LCA and LCE distributions in sediment and SPM samples

Among the 29 alkenone-containing Chinese lakes (the 8 other lakes surveyed do not contain detectable LCAs in the surface sediments) and 14 Spanish lakes (Table S1), the two most abundant chain lengths, C₃₇Me and C₃₈Et alkenones, display significant differences in distributions. C₃₇Me/C₃₈Et ratios varied from 0.09 to 5.9 with a mean value of 1.2 for sediment samples, and from 0.4 to 11.7 with a mean value of 2.2 for SPM samples (Tables S1 and S2). %C37:4 varied from 13.6% to 69.3% with a mean value of 39.2% for sediment samples, and from 12.6% to 56.0% with a mean value of 32% for SPM samples (Tables S1 and S2). The alkenoates are in significantly lower abundances (~72–98 % lower; Table S1) than alkenones in all lakes studied. Lake Balikun and Alahake contain relatively abundant extended chain length, C₄₁Me and C₄₂Et alkenones (Liao et al., 2020). Among all lakes, five oligohaline lakes (Lake Sayram, Bositeng, Wulungu, Wuliangsuhai, and Aolunnarishi) contain C_{37} tri-unsaturated isomer with $\Delta^{14,21,28}$ double bond positions (C_{37:3b}), with C_{37:3a} abundance higher than C_{37:3b} (Table S1), indicating admixture of Group 1 alkenones to Group 2 (Longo et al., 2016, 2018; Yao et al., 2020; Huang et al., 2021). Note that the relative abundances of individual C₃₇ and C₃₈ alkenones (relative to total C₃₇ and C₃₈ alkenones) in 10 oligohaline lakes (including the five lakes mentioned above; salinity < 5‰) have been reported by Yao et al. (2021) for establishing the lake RIK₃₇-salinity calibration.

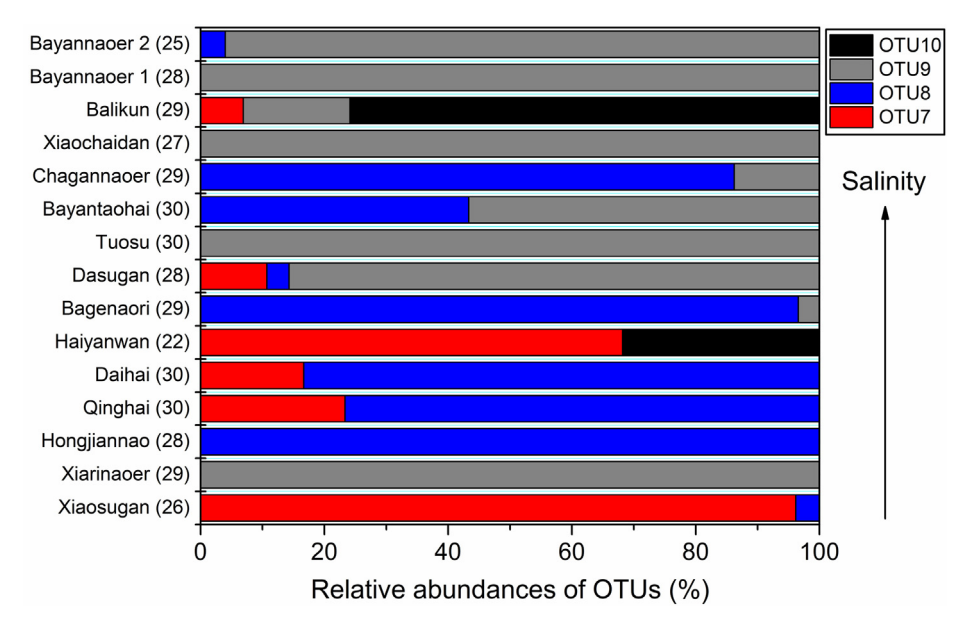


Fig. 2. (a) Relative abundances of the defined OTUs 7–10 in surface sediments of saline lakes in northern China. The number of recovered LCA-producing Isochrysidales DNA sequences from each sample is shown in brackets.

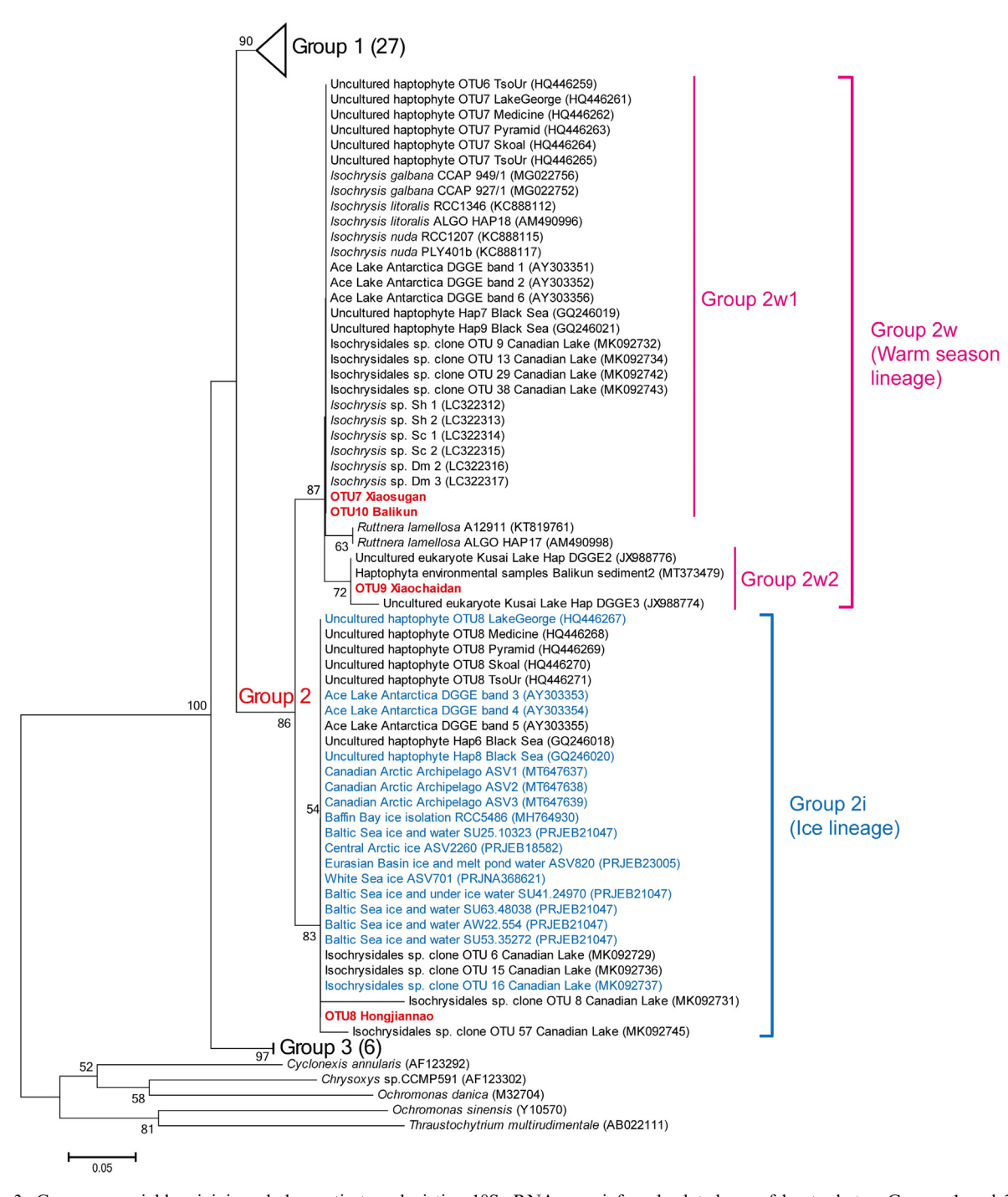


Fig. 3. Consensus neighbor-joining phylogenetic tree depicting 18S rRNA gene-inferred relatedness of haptophytes. Groups 1 and 3 are shown collapsed. Bootstrap values greater than 50% are shown at nodes. The OTUs 7–10 in this study are highlighted in red, and the Group 2i DNA sequences on the phylogenetic tree from Wang et al. (2021) are marked in blue.

4. DISCUSSION

4.1. Refined phylogenetic classifications of Group 2 Isochrysidales

Previous studies have found that there is high genetic diversity in Group 2 Isochrysidales from saline lake surface sediments (Theroux et al., 2010; Plancq et al., 2019) and

sediment cores (Coolen et al., 2004; Randlett et al., 2014). Here we divided Group 2 Isochrysidales into two phylogenetically distinct clades based on our phylogenetic tree: Group 2i (Ice lineage; Wang et al., 2021) and Group 2w (Warm season lineage) (Fig. 3). They form two distinct monophyletic groups supported respectively by 83% and 87% bootstrap values (Fig. 3). In our lake water samples collected in the summer, all recovered DNA sequences are

exclusively monopolized by Group 2w (Fig. S1), indicating that the group blooms in the relatively warm season in lake environments.

Group 2i subclade has been found in high latitude marine environments that experience seasonal sea ice coverage and certain saline lakes with seasonal or perennial ice cover (Wang et al., 2021). The spring-blooming OTU 8 (or Hap-A) from Lake George (Theroux et al., 2020) and other published saline lakes (e.g., Medicine Lake, Pyramid Lake, Skoal Lake, and Tso Ur; Theroux et al., 2010) as well as our investigated lakes is clustered within this monophyletic clade (Fig. 3). Typically, the published Antarctic Ace Lake DGGE 3-5 from sediment core (Coolen et al., 2004) and Canadian saline lake OTUs 6, 8, 15, 16, and 57 from surface sediments (Plancq et al., 2019) also share the common clade. We infer that the Group 2i commonly blooms in saline lakes in spring when lake water salinity is relatively low as a result of increased runoff from snowmelt and low temperature (hence low evaporation) (Zhao et al., 2018; Theroux et al., 2020).

Our defined Group 2w contains two subclade Groups 2w1 and 2w2, and the Group 2w2 occupies a monophyletic group that branched within the Group 2w with 72% bootstrap value (Fig. 3). The summer-blooming OTU 7 (or Hap-B) from Lake George (Theroux et al., 2020) and other published saline lakes (e.g., Medicine Lake, Pyramid Lake, Skoal Lake, and Tso Ur; Theroux et al., 2010) as well as our investigated lakes is clustered within Group 2w1, whereas our newly found OTU 9 is affiliated with Group 2w2. Typically, the published Antarctic Ace Lake DGGE 1, 2 and 6 from sediment core (Coolen et al., 2004) and the Canadian saline lake OTUs 9, 13, 29 and 38 from surface sediments (Plancq et al., 2019) fall within the Group 2w1. Group 2w may commonly bloom during the warm season in lake environments, given that our summer lake waters also exclusively host the subclade (Fig. S1).

4.2. Chemotaxonomic differences for LCAs in Groups 2i, 2w1, and 2w2 subclades

We present the typical gas chromatograms of LCAs and LCEs from surface sediments of 6 representative saline lakes (Hongjiannao, Bagenaori, Xiaosugan, Haiyanwan, Xiaochaidan, and Bayannaoer) dominated by Groups 2i, 2w1, or 2w2 subclades, respectively (Figs. 2 and 4). The lakes with different Group 2 subclades, even with the same subclades, can still show significant differences in LCA profiles, such as the relative ratios of C₃₇Me and C₃₈Et alkenones (Fig. 4). However, the relative abundance of $C_{37:4}$ alkenone shows distinct differences. The lakes with dominant Group 2i display the highest % $C_{37:4}$ (62.6% \pm 3.2; n = 2). These are followed in turn by those with the dominant Groups 2w2 (46.1% \pm 4.2; n = 2) and 2w1 (20.5%) \pm 1.1; n = 2), respectively (Fig. 4). Hongjiannao and Bagenaori with the dominant Group 2i show a remarkable predominance of C₃₇ alkenones over C₃₈ alkenones, with high abundance of C_{37:4} alkenone (Fig. 4a and 4b). The abundant C_{37:4} alkenone may, in part, be due to relatively cold temperatures experienced by the ice-related Group 2i. Although Xiaosugan and Haiyanwan share the dominant

Group 2w1, they display significant differences in LCA profiles (Fig. 4c and 4d). The LCAs from Xiaosugan are dominated by both C37:3aMe and C38:3aEt alkenones, with C_{38:3a}Et being the most abundant (Fig. 4c), which is similar to those from most of the Spanish saline lakes (Pearson et al., 2008). Whereas Haiyanwan features a profile primarily composed of C_{37·3a}Me alkenone (Fig. 4d), which is very similar to the LCA distributions from cultured Group 2w1 species I. galbana, I. litoralis, and I. nuda (Liao et al., 2020). Xiaochaidan and Bayannaoer with the dominant Group 2w2 contain almost the same abundances of C_{37:4} and C_{37:3a} alkenones (Fig. 4e and 4f), with higher C_{37:4} than that in Group 2w1. However, no isolated Group 2 species are closely related to Group 2w2 based on our phylogenetic tree (Fig. 3). Hence our observed high C_{37.4} abundance in Group 2w2 will require further confirmation from isolated cultures.

4.3. Environmental controls on presence/absence of Groups 2i, 2w1, and 2w2 subclades

We classify the Group 2 DNA sequences from surface sediments in our investigated saline lakes and other published lakes (Theroux et al., 2010; Plancq et al., 2019) into the three subclade Groups 2i, 2w1, and 2w2 based on our phylogenetic tree (Fig. 3; Table S4). Of the 25 lakes, 13 lakes contain the assemblage of Groups 2i and 2w1, 4 lakes contain the assemblage of Groups 2i and 2w2 (lower DNA abundances of Group 2i in higher salinity environments), 6 lakes contain only one subclade, and two lakes contain a main assemblage of Groups 2w1 and 2w2 (Table S4). Note that previously published saline lakes only contain the assemblage of Groups 2i and 2w1 in the relatively small salinity range of 1.7–25.2‰ (Table S4; Theroux et al., 2010; Plancq et al., 2019).

Combined with available water chemistry data (major cations and anions) from these corresponding lakes (Table S4; Wang and Dou, 1998; Galat et al., 1981; Sun et al., 2007; Zhang et al., 2009, 2015; Wu et al., 2010; Toney et al., 2012; Yang et al., 2013; Plancq et al., 2018, 2019), we performed an RDA using the relative abundances of three subclades and environmental parameters (Fig. 5). The RDA axes 1 and 2 together explain 76.1% of the variance in three subclades and 99.8% of the relationships between three subclades and environmental parameters. Axis 1 accounts for 59.3% of three subclade variances. and Group 2w2 is positively correlated with salinity and Cl. Group 2w1 appears to have more preference for K and sulfate. Interestingly, Group 2i is positively correlated with abundances of Ca²⁺, Mg²⁺, and HCO₃, probably due to increased supply of these ions derived from weathering and erosion of carbonate minerals (e.g., calcite (CaCO₃) and dolomite (CaMg(CO₃)₂) from the melt water inputs during the spring season (Romero-Mujalli et al., 2018). However, a number of potential factors (e.g., primer annealing quality, suitability/specificity of primers, and competition from other eukaryotes in lakes) can influence the recovery of the targeted DNA sequences (e.g., Coolen et al., 2004; Plancq et al., 2019; Yao et al., 2019). More quantitative genomic studies across the entire seasonal cycle

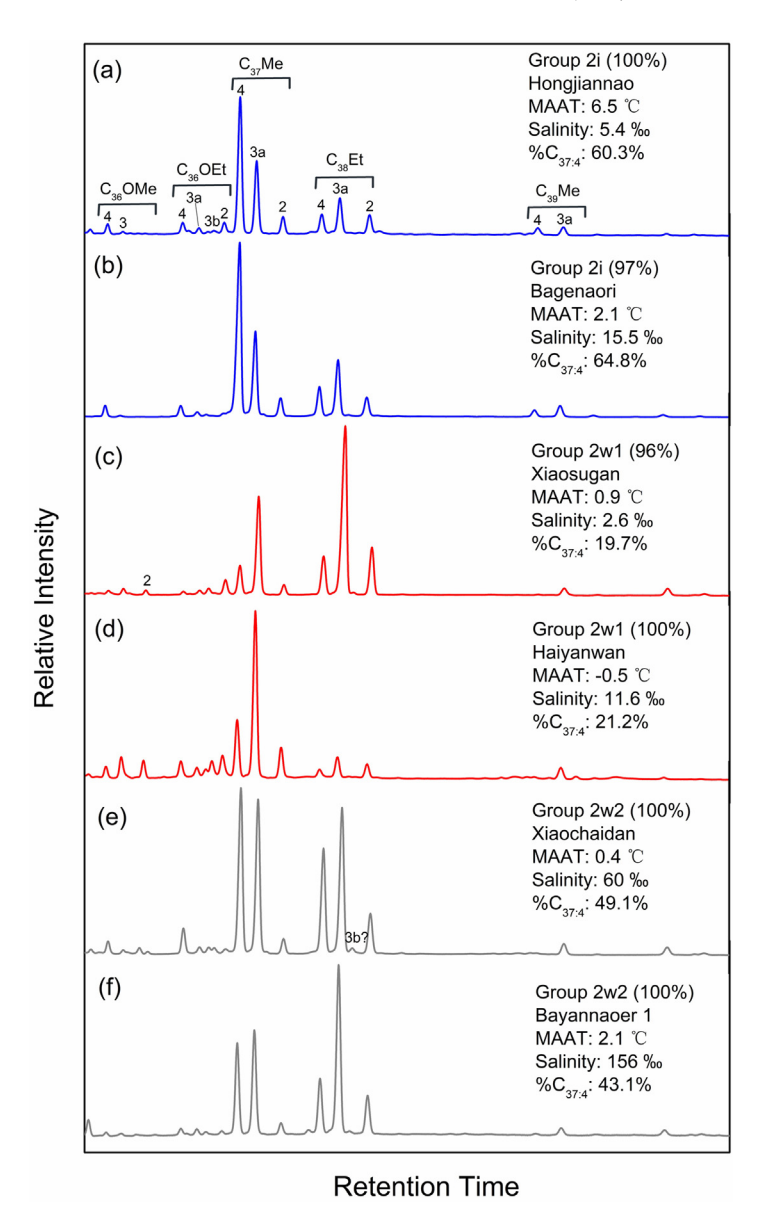


Fig. 4. Partial gas chromatograms showing typical distributions of LCAs and LCEs in surface sediments of Chinese saline lakes with dominant Groups 2i, 2w1, and 2w2 subclades.

are needed to better define environmental controls on the relative abundances of the three Group 2 subclades.

To further assess the environmental controls on the presence/absence of Groups 2i, 2w1 and 2w2, we performed logistic regressions between the categorical presence/absence of three subclades and lake water chemistry parameters using the reviewed dataset (Table S4). We define the water chemistry parameters as relatively significant factors when both p values of regression coefficients (B1 and B2) for each water chemistry factor are less than 0.5 (Table S5). The presence/absence probability of Groups 2i, 2w1 and 2w2 appears to be influenced by a combination of salinity, Na⁺, Cl⁻, CO₃⁻, especially salinity with the highest statistical significance as indicated by the lowest p values (Table S5). Groups 2i and 2w1 prefer to occur in the environmental conditions with relatively low salinity and low

abundances of Na⁺, Cl⁻ and CO₃², and Group 2i has higher probability of presence than Group 2w1 (Fig. 6). In contrast, Group 2w2 tends to occur in relatively high salinity conditions with abundant Na⁺, Cl⁻ and CO₃² (Fig. 6). Culture experiments using isolated species/strain of different Group 2 subclades would help to further constrain their salinity tolerance and preference for various cations and anions.

Together, Groups 2i, 2w1 and 2w2 subclades appear to occupy different ecological niches (Fig. 7). The Group 2i blooms the earliest in the spring. It frequently co-occurs with warm season blooming Group 2w1 in sediments from lakes with low to intermediate salinity levels. Whereas another warm season blooming Group 2w2 is well adapted to hypersaline lakes (defined here as salinity $> \sim 50\% e$) (Fig. 6d and 7).

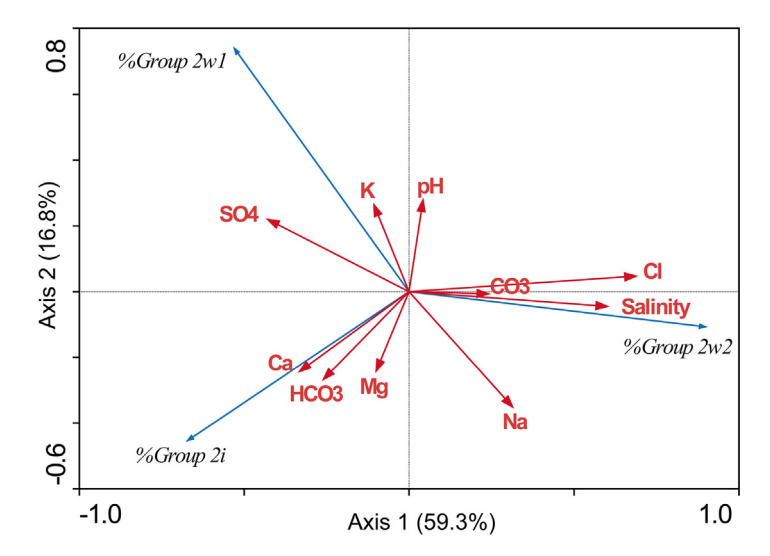


Fig. 5. RDA showing the relationships between Group 2 subclades and environmental parameters from the reviewed dataset (Table S4).

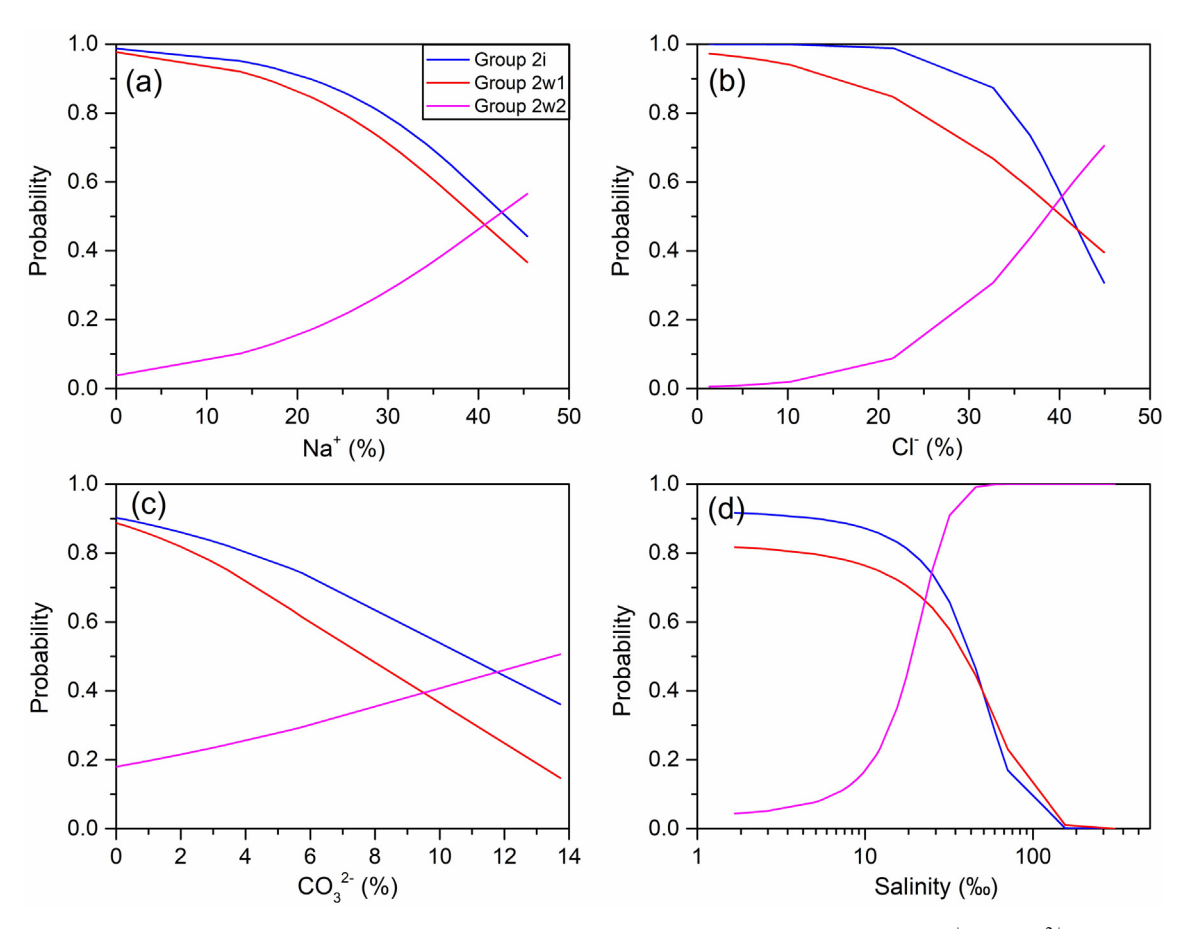


Fig. 6. Logistic probability for the presence and absence of Groups 2i, 2w1 and 2w2 along the gradient of Na^+ , $C\Gamma$, CO_3^{2+} , and salinity from the reviewed dataset (Table S4).

4.4. Constraints on the application of ${}^{6}\!\!\!/ C_{37:4}$ as a salinity proxy

The observed negative correlations between $\%C_{37:4}$ and salinity in saline lakes of the northern Qinghai-Tibetan Pla-

teau has led to the proposal that $\%C_{37:4}$ could be used as a salinity proxy on a regional scale (Table S6; Liu et al., 2008; 2011). However, culture experiments show that $\%C_{37:4}$ is positively correlated with salinity for *I. galbana* and *R. lamellosa* (Ono et al., 2012; Chivall et al., 2014; M'Boule

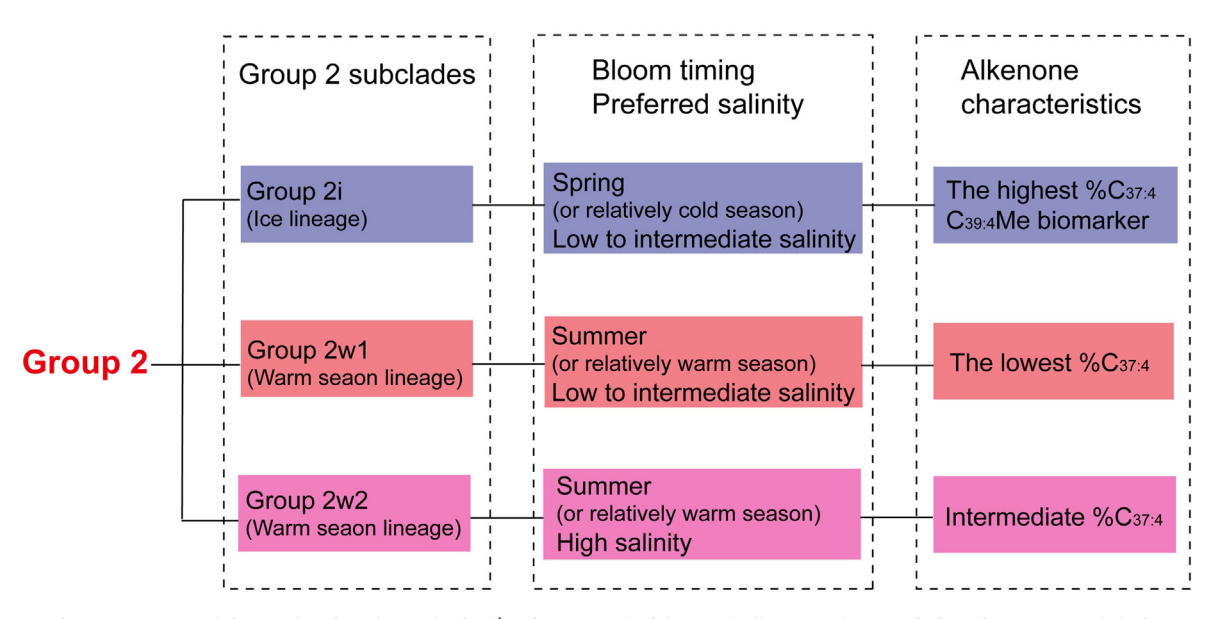


Fig. 7. Conceptual figure showing the ecological/environmental niches and alkenone characteristics of Group 2 subclades.

et al., 2014), or little influenced by salinity for Group 2i strain RCC5486 within the salinity range of ~ 10 to 40% (Wang et al., 2021). The influence of salinity on %C_{37:4} in certain regional saline lakes can be attributed to shifts in proportion of alkenones produced by different Group 2 species/clades during different seasons.

In saline lakes with moderate salinity ($< \sim 30\%$); excluding freshwater and oligohaline lakes with occurrence of Group 1 Isochrysidales), Groups 2i and 2w1 frequently co-occur with each other (Table S4) and have a higher likelihood of presence than Group 2w2 (Fig. 6d). Given the high C_{37:4} abundance of Group 2i (Fig. 4), the negative correlation between %C_{37:4} and salinity in saline lakes of the northern Qinghai-Tibetan Plateau, especially within the salinity range of $< \sim 30\%$ (Liu et al., 2008; 2011), can be mainly attributed to a decreased relative contribution of Group 2i (relative to Group 2w1) with increasing salinity. Many saline lakes have much lower salinity in the spring season due to snow melt, increased runoff and low temperature (low evaporation). For example, Lake George salinity in early spring is only $\sim 1/7$ of the peak summer salinity (Theroux et al., 2020). Therefore, higher %C_{37:4} resulting from a higher proportion of alkenones produced by Group 2i may fortuitously correlate with an overall lower average lake salinity (which, unfortunately, is rarely accurately monitored over the entire seasonal cycle). Such correlation may depend on regional winter-spring precipitation and snowmelt input to certain saline lakes with a predominance of Groups 2i and 2w1. For example, in a sediment core from Lake Gahai on the Qinghai-Tibetan plateau, %C37:4 shows a strong positive correlation with regional winterspring precipitation during the instrumental period, and has been used to reconstruct winter-spring precipitation during the past millennium (Zhao et al., 2018). Such a correlation has been interpreted as the result of an increased contribution of alkenones from Group 2i, when enhanced

In saline lakes with relatively high salinity (\sim 30%), the likelihood of Group 2w2 dominance gradually increases $(> \sim 0.6; Fig. 6d)$, indicating that Group 2w2 would likely outcompete Groups 2i and 2w1. Given that Group 2w2 also contains relatively high C_{37:4} abundance (Fig. 4), an increased contribution of Group 2w2 would increase % C_{37.4} in lake sediments as salinity continues to rise. This is opposite to the trend observed in the relatively low-tointermediate salinity lakes of the northern Qinghai-Tibetan Plateau (Liu et al., 2008; 2011). The enhanced C_{37:4} alkenone has been observed in hypersaline environments from Mediterranean solar salterns (Lopez et al., 2005) and Lake Gahai (Zhao et al., 2018). He et al. (2020) have recently shown that %C₃₇₋₄ values generally decrease as salinity increases, but increase again when salinity is higher than $\sim 50\%$ in mid-latitude Asia. They interpreted the observed high C_{37:4} abundance in the hypersaline lakes to result from the contribution of spring LCA production, as spring meltwater could lead to a significant decrease in lake water salinity, especially in shallow (and small) lakes (He et al., 2020). Our statistical analyses of DNA data, however, indicate that the spring-blooming Group 2i has a very low likelihood of presence ($< \sim 0.2$) in such hypersaline lakes (Fig. 6d). Therefore, in high salinity lakes, input of alkenones from Group 2w2 could further complicate the relationship between %C_{37:4} and salinity. Specifically, %C_{37:4} would increase with increasing salinity as Group 2w2 contribution increases in high salinity waters. Thus, in lakes where alkenones are primarily produced by Group 2w1 and 2w2 Isochrysidales, the correlation between $%C_{37:4}$ and salinity may have the opposite trend to that in lakes where alkenones are primarily produced by Group 2i and 2w1 Isochrysidales.

4.5. Chemotaxonomic biomarker for the ice-related Group 2i

We carefully compared the LCA and LCE distributions in surface sediments from 6 representative saline lakes, where one of the Groups 2i, 2w1, and 2w2 subclades is the dominate alkenone producer (Fig. 4). The lakes with the dominant Groups 2w1 and 2w2 do not contain C_{39.4} methyl (C_{39:4}Me) alkenone, whereas the lakes with the dominant Group 2i contain this compound (Fig. 4). Overall, %C_{39.4}Me values synchronously increase with increasing relative abundance of Group 2i DNA sequences in the surface sediments of our study lakes (Fig. 8a), indicating that a greater contribution from Group 2i leads to higher abundance of C_{39:4}Me alkenone in the sediments. Importantly, the cultured Group 2i strain RCC5486 (Wang et al., 2021) also produces the abundant C_{39:4}Me (Fig. 8b). In contrast, other Group 2w species (including I. galbana, I. litoralis, I. nuda, R. lamellosa, and unclassified

strain Sh1, Sc2 and Dm2 isolated from Canadian saline lakes; Fig. 3) have not been observed to produce $C_{39:4}$ Me alkenone, even in relatively cold temperatures (4–10 °C) (Fig. 8b, Table S7; Nakamura et al., 2014; Araie et al., 2018; Zheng et al., 2019; Liao et al., 2020), with the exception of two data from *I. nuda* at 4 °C and *I. litoralis* at 15 °C producing trace amounts of $C_{39:4}$ Me (Table S7; Liao et al., 2020). The $C_{39:4}$ Me alkenone may thus be produced predominantly by Group 2i in saline lake environments. Therefore, we propose that $C_{39:4}$ Me alkenone could be used as an indicator for the contribution of Group 2i. Higher % $C_{39:4}$ Me values may reflect a greater input of a spring (or relatively cold season) temperature signal derived from the Group 2i in lake sediments.

4.6. Potential summer temperature proxy based on the ratio of alkenones and alkenoates

We compiled the previously published U_{37}^K , $U_{37}^{K'}$, and $U_{37}^{K''}$ datasets from 11 cultured Group 2 species/strains (Table S8; Sun et al., 2007; Nakamura et al., 2014; Araie

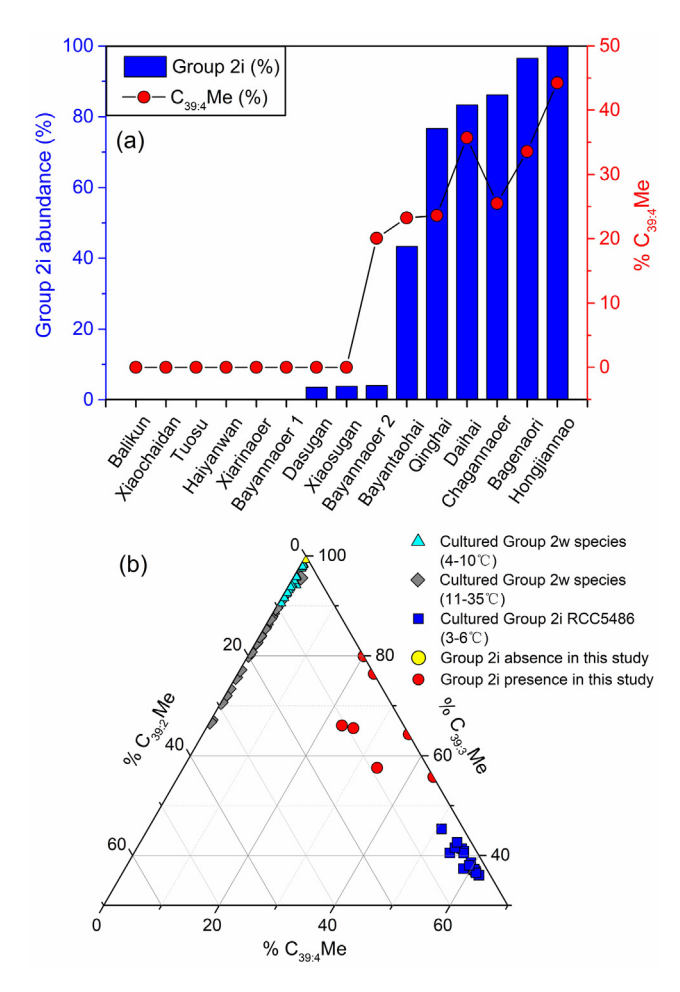


Fig. 8. (a) %C_{39:4}Me vs. relative abundance of Group 2i DNA sequences (relative to total Group 2 DNA sequences). (b) Ternary diagram showing the C₃₉Me distributions from surface sediments with the presence and absence of Group 2i in this study, as well as cultured Group 2i strain RCC5486 and Group 2w species under relatively cold temperature (4–10 °C) and warm temperature (11–35 °C) (Table S7; Nakamura et al., 2014; Araie et al., 2018; Zheng et al., 2019; Liao et al., 2020).

et al., 2018; Zheng et al., 2019; Liao et al., 2020), SPM samples of Lake George and Lake Qinghai (Table S9; Toney et al., 2010; Wang and Liu, 2013), and surface sediment samples of globally distributed saline lakes (Table S10: Chu et al., 2005; Pearson et al., 2008; Toney et al., 2010; Liu et al., 2011; Zhao et al., 2014; Song et al., 2016; Plancq et al., 2018; He et al., 2020). The U_{37}^{K} , $U_{37}^{K'}$, and $U_{27}^{K''}$ values of each cultured Group 2 species/strain are significantly correlated with growth temperatures, but the yintercepts and/or slopes for these temperature calibrations are highly variable (y-intercept: -1.077- -0.158 for U_{37}^{K} , -0.599 –0.0419 for $U_{37}^{K^{\prime}},$ –0.08 –0.584 for $U_{37}^{K^{\prime\prime}}$; slope: 0.0195–0.0473 for $U_{37}^{K},$ 0.0016–0.0377 for $U_{37}^{K},$ 0.014 – 0.042 for $U_{37}^{K''}$; Figs. S2a-2c; Table S11). This indicates that different Group 2 species, even strains, have very different physiological responses to temperature variations. However, there are no relationships between U_{37}^K ($U_{37}^{K'}$ and $U_{37}^{K''}$) values and temperatures for all compiled SPM and surface sediment samples of global saline lakes, although the linear correlation between $U_{37}^{K''}$ and in situ water temperatures is better than U_{37}^{K} and $U_{37}^{K'}$ for SPM samples from Lake George (Figs. S2d-2i).

We find that C₃₈Et/C₃₆OEt values of our SPM samples are significantly correlated with in situ water temperatures (Fig. 9b). In our compiled dataset from cultured Group 2 species (Table S8), C₃₈Et/C₃₆OEt values of two common species R. lamellosa and I. galbana also display similar behaviors in their physiological response to temperatures (Fig. 9a), and all Group 2 species show overall increase in C₃₈Et/C₃₆OEt with increasing temperature (Fig. S3). For the surface sediments that integrate different seasonal production of LCAs and LCEs, the presence of C_{30.4}Me alkenone indicates that the spring (or relatively cold season) temperature signal derived from Group 2i overprints the LCA and LCE signatures. After excluding the samples with C_{39.4}Me, C₃₈Et/C₃₆OEt values are correlated with both MAAT and mean summer air temperatures (MSAT) (Fig. 9c and 9d). Importantly, the correlation coefficient $(R^2 = 0.731)$ of $C_{38}Et/C_{36}OEt$ with MSAT is stronger than that $(R^2 = 0.414)$ with MAAT, indicating that $C_{38}Et/$ C₃₆OEt better reflects the summer temperature signal derived from Group 2w blooming in the relatively warm

Therefore, we provide one potential solution for disentangling mixed inputs from Group 2 subclades in sediment records. The presence of C_{39:4}Me alkenone in lake sediments would indicate that alkenone-inferred temperatures

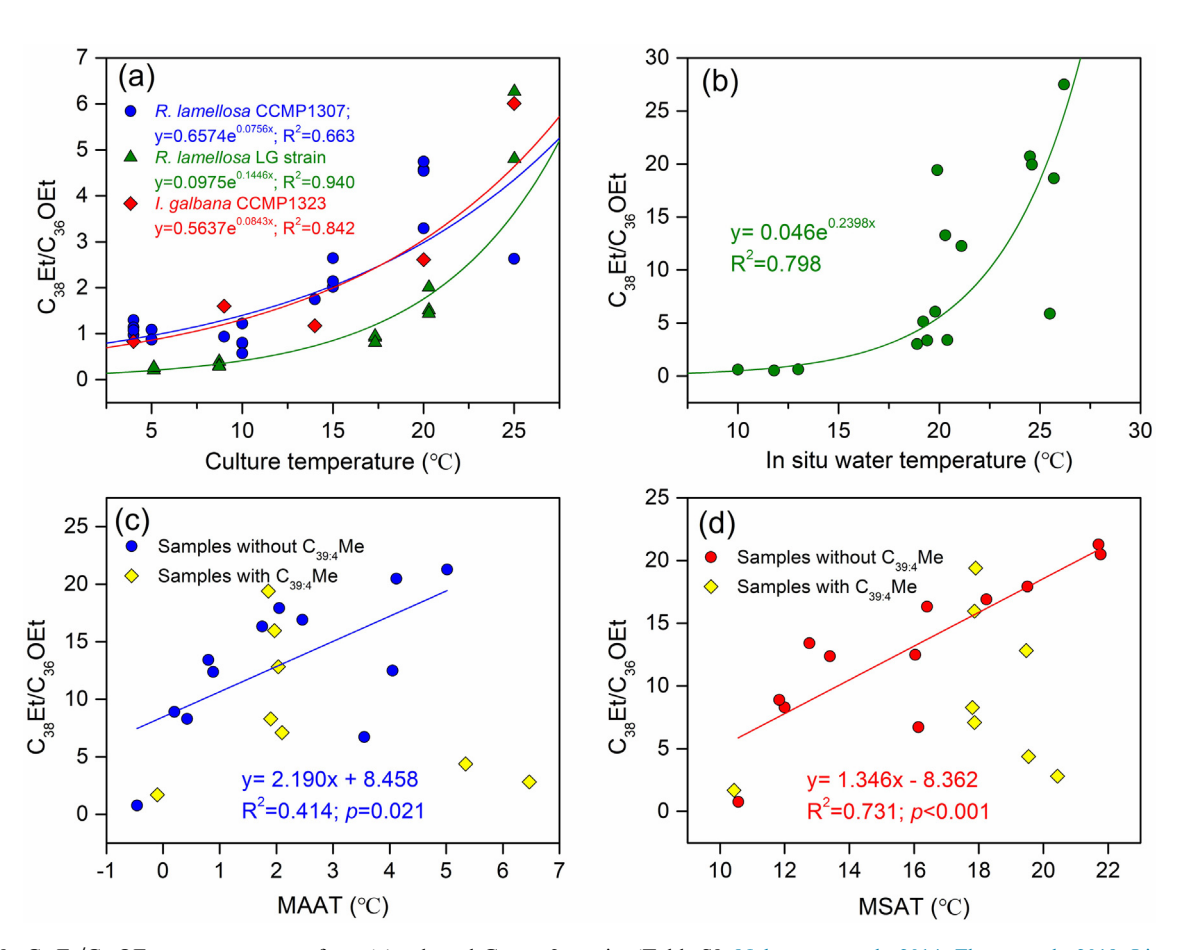


Fig. 9. C₃₈Et/C₃₆OEt vs. temperatures from (a) cultured Group 2 species (Table S9; Nakamura et al., 2014; Zheng et al., 2019; Liao et al., 2020), (b) SPM and (c and d) surface sediment samples of Chinese saline lakes in this study. The surface sediment samples that contain alkenone isomers from mixed Group 1/2 Isochrysidales are not used for this analysis.

contain the imprint of spring season temperature signal derived from Group 2i Isochrysidales. Group 2i is commonly found in association with Group 2wl Isochrysidales which blooms during the summer. The mixed alkenone production by Group 2i and 2wl complicates the interpretation of inferred temperatures for two reasons: 1) the two subclades bloom during different seasons and experience different growth temperatures (i.e., Group 2i experiences lower growth temperatures than 2wl); and 2) they yield different alkenone profiles and have large differences in temperature calibrations (Figs. S2a-2c). However, if the sample does not contain C_{39:4}Me (suggesting an absence of Group 2i contribution), summer temperatures could be reconstructed using C₃₈Et/C₃₆OEt.

Alternatively, unsaturation ratios of extended C₄₁Me and C₄₂Et alkenones have recently been proposed as a summer/warm season temperature proxy in certain hypersaline lakes (Liao et al., 2020). Systematic analyses of Isochrysidales cultures demonstrate that common Group 2 species (I. galbana, I. litoralis, I. nuda, and R. lamellosa) can all produce variable amounts of these extended alkenones. However, the amounts of C41Me and C42Et alkenones produced by different Group 2 species are highly variable, with I. nuda producing 400 to 600% higher amounts than other species. It is possible that extended C₄₁Me and C₄₂Et alkenones are mostly produced by a limited number of warm season Group 2 species in saline lakes, particularly those that are more adapted to relatively high salinity waters (Liao et al., 2020). Thus, the use of unsaturation ratios of C₄₁Me and C₄₂Et alkenones for paleotemperature reconstructions could reduce the impact of the species mixing problem in saline lakes (Liao et al., 2020). For example, C₄₁Me and C₄₂Et inferred temperatures using surface sediments from Lake Balikun and Alahake match closely with instrumental summer season temperatures (Liao et al., 2020), but C_{37} alkenone-inferred temperatures are up to 18 °C colder. Therefore, if present in sufficient abundance in sediments, C41Me and C42Et alkenones are potentially excellent candidates for reconstructing past warm season temperatures.

5. CONCLUSIONS

In this study, we combine genomic, ecological and lipid biomarker data to examine the underlying environmental controls on LCAs and LCEs in saline lakes spanning a wide range of salinity (0.5-308%). We classify Group 2 Isochrysidales into three subclades: one ice-related Group 2i and two warm season-blooming Groups 2w1 and 2w2. Groups 2i and 2w1 flourish in relatively low to intermediate salinity waters, whereas Group 2w2 thrives in hypersaline waters. We show that %C_{37:4} in saline lake sediments cannot simply be used as a salinity proxy without taking into consideration the assemblages of different Group 2 subclades. Group 2i produces the highest relative abundance of C_{37:4} alkenone, followed in turn by Groups 2w2 and 2w1 respectively. Depending on winter-spring precipitation and snowmelt input, %C37:4 may occasionally record overall salinity changes (with higher %C37:4 corresponding to lower salinity) in saline lakes with a dominance of Groups 2i and 2w1. However, in saline lakes where Group 2i is absent, the relationship between $\%C_{37:4}$ and salinity can be more complicated. For example, higher $\%C_{37:4}$ may correspond to higher salinity in lakes with a dominance of Group 2w1 and 2w2.

Based on our compiled data, C_{39:4}Me alkenone appears to be a chemotaxonomic biomarker for Group 2i. The presence of C_{39:4}Me alkenone in lake sediments indicates a possible influence of spring (or relatively cold season) temperature signal derived from Group 2i. When sediment samples containing C_{39:4}Me are excluded in the lakes studied, the C₃₈Et/C₃₆OEt from surface sediments correlates strongly to summer temperatures. We propose that C₃₈Et/C₃₆OEt could be used to reconstruct past summer temperature changes in samples that do not contain $C_{39:4}$ Me alkenone. Alternatively, if C_{41} and C_{42} alkenones are present in sufficient abundance for accurate measurements, unsaturation ratios of C41 and C42 alkenones could be used for summer temperature reconstructions in saline lakes, as only a limited number of Group 2w species (such as I. nuda) are known to produce large quantities of these extended alkenones (Liao et al., 2020).

Declaration of Competing Interest

The authors declare that they have no known competing financial interests or personal relationships that could have appeared to influence the work reported in this paper.

ACKNOWLEDGMENTS

This work was supported by the National Natural Science Foundation of China (Nos. 42073070; 41702187), the U.S. National Science Foundation (Nos. EAR-1122749, PLR-1503846, EAR-1502455, EAR-1762431), and the Fundamental Research Funds for the Central Universities (Nos. xxj032020004). YH thanks Swiss Federal Institue of Technology for a visiting professorship and a senior fellowship at Collegium Helveticum in fall of 2021. We thank J. Jing and J. Chen for assistance during sample collection and pretreatment, and K. Wang for providing the Group 2i DNA sequences. We are also grateful for the comments from three anonymous reviewers that helped us improve the manuscript.

APPENDIX A. SUPPLEMENTARY DATA

Supplementary data to this article can be found online at https://doi.org/10.1016/j.gca.2021.11.001.

REFERENCES

Aponte J. C., Dillon J. T. and Huang Y. (2013) The unique liquid chromatographic properties of Group II transition metals for the separation of unsaturated organic compounds. *J. Sep. Sci.* 36, 2563–2570.

Araie H., Nakamura H., Toney J. L., Haig H. A., Plancq J., Shiratori T., Leavitt P. R., Seki O., Ishida K., Sawada K., Suzuki I. and Shiraiwa Y. (2018) Novel alkenone-producing strains of genus Isochrysis (Haptophyta) isolated from Canadian saline lakes show temperature sensitivity of alkenones and alkenoates. *Org. Geochem.* 121, 89–103.

- Brassell S. C., Eglinton G., Marlowe I. T., Pflaumann U. and Sarnthein M. (1986) Molecular stratigraphy: a new tool for climatic assessment. *Nature* 320, 129–133.
- Chivall D., M'Boule D., Sinke-Schoen D., Sinninghe Damsté J. S., Schouten S. and van der Meer M. T. J. (2014) Impact of salinity and growth phase on alkenone distributions in coastal haptophytes. *Org. Geochem.* **67**, 31–34.
- Chu G., Sun Q., Li S., Zheng M., Jia X., Lu C., Liu J. and Liu T. (2005) Long-chain alkenone distributions and temperature dependence in Lacustrine surface sediments from China. *Geochim. Cosmochim. Acta* 69, 4985–5003.
- Conte M. H., Thompson A., Lesley D. and Harris R. P. (1998) Genetic and physiological influences on the alkenone/alkenoate versus growth temperature relationship in *Emiliania huxleyi* and *Gephyrocapsa oceanica*. *Geochim. Cosmochim. Acta* 62, 51–68.
- Conte M. H., Sicre M., Ruhlemann C., Weber J. C., Schulte S., Schulz-Bull D. and Blanz T. (2006) Global temperature calibration of the alkenone unsaturation index (U37K') in surface waters and comparison with surface sediments. *Geochem. Geophy. Geosy.* 7.
- Coolen M. J. L., Muyzer G., Rijpstra W. I. C., Schouten S., Volkman J. K. and Damsté Sinninghe J. S. (2004) Combined DNA and lipid analyses of sediments reveal changes in Holocene haptophyte and diatom populations in an Antarctic lake. *Earth Planet. Sc. Lett.* 223, 225–239.
- Coolen M. J. L., Saenz J. P., Giosan L., Trowbridge N. Y., Dimitrov P., Dimitrov D. and Eglinton T. I. (2009) DNA and lipid molecular stratigraphic records of haptophyte succession in the Black Sea during the Holocene. *Earth Planet. Sc. Lett.* 284, 610–621.
- D'Andrea W. J. and Huang Y. (2005) Long chain alkenones in Greenland lake sediments: Low δ^{13} C values and exceptional abundance. *Org. Geochem.* **36**, 1234–1241.
- D'Andrea W. J., Lage M., Martiny J. B. H., Laatsch A. D., Amaral-Zettler L. A., Sogin M. L. and Huang Y. (2006) Alkenone producers inferred from well-preserved 18S rDNA in Greenland lake sediment. *J. Geophys. Res.* 111.
- D'Andrea W. J., Huang Y., Fritz S. C. and Anderson N. J. (2011) Abrupt Holocene climate change as an important factor for human migration in West Greenland. *Proc. Natl. Acad. Sci.* 108, 9765–9769.
- D'Andrea W. J., Theroux S., Bradley E. S. and Huang X. (2016) Does phylogeny control U37K -temperature sensitivity? Implications for lacustrine alkenone paleothermometry. *Geochim. Cosmochim. Acta* 175, 168–180.
- Dillon J. T., Long W. M., Zhang Y., Torozo R. and Huang Y. (2016) Identification of double-bound positions in isomeric alkenones from a lacustrine haptophyte. *Rapid Commun. Mass Spectrom.* 30, 112–118.
- Eglinton G., Bradshaw S. A., Rosell A., Sarnthein M., Pflaumann U. and Tiedemann R. (1992) Molecular record of secular sea surface temperature changes on 100-year timescales for glacial terminations I, II, IV. *Nature* **356**, 423–426.
- Fick S. E. and Hijmans R. J. (2017) WorldClim 2: new 1-km spatial resolution climate surfaces for global land areas. *Int. J. Climatol.* 37, 4302–4315.
- Galat D. L., Lider E. L., Vigg S. and Robertson S. R. (1981) Limnology of a large, deep, North American terminal lake, Pyramid Lake, Nevada, U.S.A. *Hydrobiologia* 81, 281–317.
- He Y., Zhao C., Wang Z., Wang H., Song M., Liu W. and Liu Z. (2013) Late Holocene coupled moisture and temperature changes on the northern Tibetan Plateau. *Quaternary Sci. Rev.* 80, 47–57.
- He Y., Wang H., Meng B., Liu H., Zhou A., Song M., Kolpakova M., Krivonogov S., Liu W. and Liu Z. (2020) Appraisal of

- alkenone- and archaeal ether-based salinity indicators in midlatitude Asian lakes. *Earth Planet. Sc. Lett.* **538** 116236.
- Huang Y., Zheng Y., Heng P., Giosan L. and Coolen M. J. L. (2021) Black Sea paleosalinity evolution since the last deglaciation reconstructed from alkenone-inferred Isochrysidales diversity. Earth Planet. Sc. Lett. 564 116881.
- Hou J., Huang Y., Zhao J., Liu Z., Colman S. and An Z. (2016) Large Holocene summer temperature oscillations and impact on the peopling of the northeastern Tibetan Plateau. *Geophys. Res. Lett.* 43.
- Hou W., Dong H., Li G., Yang J., Coolen M. J. L., Liu X., Wang S., Jiang H., Wu X., Xiao H., Lian B. and Wan Y. (2014) Identification of photosynthetic plankton communities using sedimentary ancient DNA and their response to late-Holocene climate change on the Tibetan Plateau. *Sci. Rep.* 4, 6648.
- Kaiser J., Wang K. J., Rott D., Li G., Zheng Y., Amaral-Zettler L., Arz H. W. and Huang Y. (2019) Changes in long chain alkenone distributions and Isochrysidales groups along the Baltic Sea salinity gradient. Org. Geochem. 127, 92–103.
- Liao S., Yao Y., Wang L., Wang K. J., Amaral-Zettler L., Longo W. M. and Huang Y. (2020) C₄₁ methyl and C₄₂ ethyl alkenones are biomarkers for Group II Isochrysidales. *Org. Geochem.* 147 104081.
- Liu W., Liu Z., Fu M. and An Z. (2008) Distribution of the C₃₇ tetra-unsaturated alkenone in Lake Qinghai, China: A potential lake salinity indicator. *Geochim. Cosmochim. Acta* 72, 988–997.
- Liu W., Liu Z., Wang H., He Y., Wang Z. and Xu L. (2011) Salinity control on long-chain alkenone distributions in lake surface waters and sediments of the northern Qinghai-Tibetan Plateau, China. Geochim. Cosmochim. Acta 75, 1693–1703.
- Liu Z., Henderson A. C. G. and Huang Y. (2006) Alkenone-based reconstruction of late-Holocene surface temperature and salinity changes in Lake Qinghai, China. Geophys. Res. Lett. 33.
- Longo W. M., Dillon J. T., Tarozo R., Salacup J. M. and Huang Y. (2013) Unprecedented separation of long chain alkenones from gas chromatography with a poly (trifluoropropylmethylsiloxane) stationary. *Org. Geochem.* 65, 94–102.
- Longo W. M., Theroux S., Gibin A. E., Zheng Y., Dillon J. T. and Huang Y. (2016) Temperature calibration and phylogenetically distinct distributions for freshwater alkenones: Evidence from northern Alaskan lakes. *Geochim. Cosmochim. Acta* 180, 177–
- Longo W. M., Huang Y., Yao Y., Zhao J., Giblin A. E., Wang X., Zech R., Haberzettl T., Jardillier L., Toney J., Liu Z. H., Krivonogov S., Kolpakova M., Chu G. Q., D'Andrea W. J., Harada N., Nagashima K., Sato M., Yonenobu H., Yamada K., Gotanda K. and Shinozuka Y. (2018) Widespread occurrence of distinct alkenones from Group I haptophytes in freshwater lakes: Implications for paleotemperature and paleoenvironmental reconstructions. Earth Planet. Sc. Lett. 492, 239–250.
- Longo W. M., Huang Y., Russell J. M., Morrill C., Daniels W. C., Giblin A. E. and Crowther J. (2020) Insolation and greenhouse gases drove Holocene winter and spring warming in Arctic Alaska. *Quaternary Sci. Rev.* 242 106438.
- Lopez J. F., de Oteyza T. G., Teixidor P. and Grimalt J. O. (2005) Long chain alkenones in hypersaline and marine coastal microbial mats. *Org. Geochem.* 36, 861–872.
- Marlowe I. T., Green J. C., Neal A. C., Brassell S. C., Eglinton G. and Course P. A. (1984) Long chain (*n*-C₃₇-C₃₉) alkenones in the Prymnesiophyceae. Distribution of alkenones and other lipids and their taxonomic significance. *Br. Phycol. J.* **19**, 203–216.
- M'boule D., Chivall D., Sinke-Schoen D., Sinninghe Damsté J. S., Schouten S. and van der Meer M. T. J. (2014) Salinity dependent hydrogen isotope fractionation in alkenones pro-

- duced by coastal and open ocean haptophyte algae. *Geochim. Cosmochim. Acta* **130**, 126–135.
- Nakamura H., Sawada K., Araie H., Suzuki I. and Shiraiwa Y. (2014) Long chain alkenes, alkenones and alkenoates produced by the haptophyte alga Chrysotila lamellosa CCMP1307 isolated from a salt marsh. Org. Geochem. 66, 90–97.
- Ono M., Sawade K., Shiraiwa Y. and Kubota M. (2012) Changes in alkenone and alkenoate distributions during acclimatization to salinity change in *Isochrysis galbana*: Implication for alkenone-based paleosalinity and paleothermometry. *Geochem. J.* 46, 235–247.
- Pearson E. J., Juggins S. and Farrimond P. (2008) Distribution and significance of long-chain alkenones as salinity and temperature indicators in Spanish saline lake sediments. *Geochim. Cos*mochim. Acta 72, 4035–4046.
- Plancq J., Cavazzin B., Juggins S., Haig H. A., Leavitt P. R. and Toney J. L. (2018) Assessing environmental controls on the distribution of long-chain alkenones in the Canadian Prairies. Org. Geochem. 117, 43–55.
- Plancq J., Couto J. M., Ijaz U. Z., Leavitt P. R. and Toney J. L. (2019) Next-generation sequencing to identify lacustrine haptophytes in the Canadian Prairies: significance for temperature proxy applications. J. Geophys. Res-Biogeo. 124, 2144–2158.
- Prahl F. G. and Wakeham S. G. (1987) Calibration of unsaturation patterns in long-chain ketone compositions for palaeotemperature assessment. *Nature* 330, 367–369.
- Randlett M.-È., Coolen M. J. L., Stockhecke M., Pickarski N., Litt T., Balkema C., Kwiecien O., Tomonaga Y., Wehrli B. and Schubert C. J. (2014) Alkenone distribution in Lake Van sediment over the last 270 ka: influence of temperature and haptophyte species composition. *Quaternary Sci. Rev.* 104, 53–62.
- Richter N., Longo W. M., George S., Shipunova A., Huang Y. and Amaral-Zettler L. (2019) Phylogenetic diversity in freshwaterdwelling Isochrysidales haptophytes with implications for alkenone production. *Geobiology* 17, 272–280.
- Romero-Mujalli G., Hartmann J. and Börker J. (2018) Temperature and CO₂ dependency of global carbonate weathering fluxes–Implications for future carbonate weathering research. *Chem. Geol.* **527**, 118874.
- Rosell-Melé A. (1998) Interhemispheric appraisal of the value of alkenone indices as temperature and salinity proxies in high-latitude locations. *Paleoceanography* **13**, 694–703.
- Schloss P. D. and Handelsman J. (2005) Introducing DOTUR, a computer program for defining operational taxonomic units and estimating species richness. *Appl. Environ. Microb.* 71, 1501–1506.
- Simon M., López-García P., Moreira D. and Jardillier L. (2013) New haptophyte lineages and multiple independent colonizations of freshwater ecosystems. *Env. Microbiol. Rep.* 5, 322–332.
- Song M., Zhou A., He Y., Zhao C., Wu J., Zhao Y., Liu W. and Liu Z. (2016) Environmental controls on long-chain alkenone occurrence and compositional patterns in lacustrine sediments, northwestern China. *Org. Geochem.* 91, 43–53.
- Sun Q., Chu G., Liu G., Li S. and Wang X. (2007) Calibration of alkenone unsaturation index with growth temperature for a lacustrine species, *Chrysotila lamellosa* (Haptophyceae). *Org. Geochem.* 38, 1226–1234.
- Theroux S., D'Andrea W. J., Toney J., Amaral-Zettler L. and Huang Y. (2010) Phylogenetic diversity and evolutionary relatedness of alkenone-producing haptophyte algae in lakes: Implications for continental paleotemperature reconstructions. *Earth Planet. Sc. Lett.* **300**, 311–320.
- Theroux S., Huang Y., Toney J. L., Andersen R., Nyren P., Bohn R., Salacup J., Murphy L. and Amaral-Zettler L. (2020) Successional blooms of alkenone-producing haptophytes in

- Lake George, North Dakota: Implications for continental paleoclimate reconstructions. *Limnol. Oceanogr.* **65**, 413–425.
- Toney J. L., Huang Y., Fritz S. C., Baker P. A., Grimm E. and Nyren P. (2010) Climatic and environmental controls on the occurrence and distributions of long chain alkenones in lakes of the interior United States. *Geochim. Cosmochim. Acta* 74, 1563–1578.
- Toney J. L., Theroux S., Andersen R. A., Coleman A., Amaral-Zettler L. and Huang Y. (2012) Culturing of the first 37:4 predominant lacustrine haptophyte: Geochemical, biochemical, and genetic implications. *Geochim. Cosmochim. Acta* 78, 51–64.
- Volkman J. K., Eglinton G., Corner E. D. S. and Forsberg T. E. V. (1980) Long-chain alkenes and alkenones in the marine coccolithophorid *Emiliania huxleyi*. *Phytochemistry* 19, 2619– 2622.
- Wang K. J., Huang Y., Majaneva M., Belt S. T., Liao S., Novak J.,
 Kartzinel T. R., Herbert T. D., Richter N. and Cabedo-Sanz P.
 (2021) Group 2i Isochrysidales produce characteristic alkenones reflecting sea ice distribution. *Nat. Commun.* 12, 15.
- Wang L., Long W. M., Dillon J. T., Zhao J., Zheng Y., Moros M. and Huang Y. (2019) An efficient approach to eliminate steryl ethers and miscellaneous esters/ketones for gas chromatographic analysis for alkenones and alkenoates. *J. Chromatogr. A* 1596, 175–182.
- Wang S. and Dou H. (1998) *Chinese Lakes*, first ed. Science Press, Beijing.
- Wang Z. and Liu W. (2013) Calibration of the U37K' index of long-chain alkenones with the in-situ water temperature in Lake Oinghai in the Tibetan Plateau. *Chinese Sci. Bull.* 58, 803–808.
- Wang Z., Liu Z., Zhang F., Fu M. and An Z. (2015) A new approach for reconstruction Holocene temperatures from a multi-species long chain alkenone record from Lake Qinghai on the northeastern Tibetan Plateau. Org. Geochem. 88, 50–58.
- Wu Y., Li S., Lücke A., Wünnemann B., Zhou L., Reimer P. and Wang S. (2010) Lacustrine radiocarbon reservoir ages in Co Ngoin and Zigê Tangco, central Tibetan Plateau. *Quatern. Int.* 212, 21–25.
- Yang J., Jiang H., Dong H., Wang H., Wu G., Hou W., Liu W., Zhang C., Sun Y. and Lai Z. (2013) amoA-encoding archaea and thaumarchaeol in the lakes on the northeastern Qinghai-Tibetan Plateau, China. Front. Microbiol. 4, 1–17.
- Yao Y., Zhao J., Longo W. M., Li G., Wang X., Vachula R. S., Wang K. J. and Huang Y. (2019) New insights into environmental controls on the occurrence and abundance of Group I alkenones and their paleoclimate applications: evidence from volcanic lakes of northeastern China. *Earth Planet. Sc. Lett.* 527 115792.
- Yao Y., Lan J., Zhao J., Vachula R. S., Xu H., Cai Y., Cheng H. and Huang Y. (2020) Abrupt freshening since the early Little Ice Age in Lake Sayram of arid central Asia inferred from an alkenone isomer proxy. *Geophys. Res. Lett.* 47 e2020GL089257.
- Yao Y., Huang Y., Zhao J., Wang L., Ran Y., Liu W. and Cheng H. (2021) Permafrost thaw induced abrupt changes in hydrology and carbon cycling in Lake Wudalianchi, northeastern China. Geology 49, 1117–1121.
- Zhang F., Jin Z., Yu J., Zhou Y. and Zhou L. (2015) Hydrogeochemical processes between surface and groundwaters on the northeastern Chinese Loess Plateau: Implications for water chemistry and environmental evolutions in semi-arid regions. J. Geochem. Explor. 159, 115–128.
- Zhang J., Holmes J. A., Chen F., Qiang M., Zhou A. and Chen S. (2009) An 850-year ostracod-shell trace-element record of from Sugan Lake, northern Tibetan Plateau, China: Implications for interpreting the shell chemistry in high-Mg/Ca waters. *Quatern. Int.* 194, 119–133.

- Zhao J., An C., Longo W. M., Dillon J. T., Zhao Y., Shi C., Chen Y. and Huang Y. (2014) Occurrence of extended chain length C₄₁ and C₄₂ alkenones in hypersaline lakes. *Org. Geochem.* 75, 48–53.
- Zhao J., An C., Huang Y., Morrill C. and Chen F. (2017) Contrasting early Holocene temperature variations between monsoonal East Asia and westerly dominated Central Asia. *Quaternary Sci. Rev.* 178, 14–23.
- Zhao J., Thomas E. K., Yao Y., DeAraujo J. and Huang Y. (2018) Major increase in winter and spring precipitation during the Little Ice Age in the westerly dominated northern Qinghai-Tibetan Plateau. *Quaternary Sci. Rev.* 199, 30–40.
- Zheng Y., Huang Y., Andersen R. A. and Amaral-Zettler L. A. (2016) Excluding the diunsaturated alkenone in the U37K index strengthens temperature correlation for the common lacustrine and brackish-water haptophytes. *Geochim. Cosmochim. Acta* 175, 36–46.

- Zheng Y., Tarozo R. and Huang Y. (2017) Optimizing chromatographic resolution for simultaneous quantification of long chain alkenones, alkenoates and their double bond positional isomers. *Org. Geochem.* **111**, 136–143.
- Zheng Y., Heng P., Conte M. H., Vachula R. S. and Huang Y. (2019) Systematic chemotaxonomic profiling and novel pale-otemperature indices based on alkenones and alkenoates: Potential for disentangling mixed species input. *Org. Geochem.* 128, 26–41.
- Zink K. G., Leythaeuser D., Melkonian M. and Schwark L. (2001) Temperature dependency of long-chain alkenone distributions in Recent to fossil limnic sediments and in lake waters. *Geochim. Cosmochim. Acta* 65, 253–265.

Associate editor: Aaron F. Diefendorf